Tuning the crystalline phases of poly(vinylidene fluoride) for capacitive energy storage applications

Meereboer, Niels Laurens

Chapter 6

Relaxor ferroelectric behavior in P(VDF-*ter*-TrFE-*ter*-VA) terpolymers

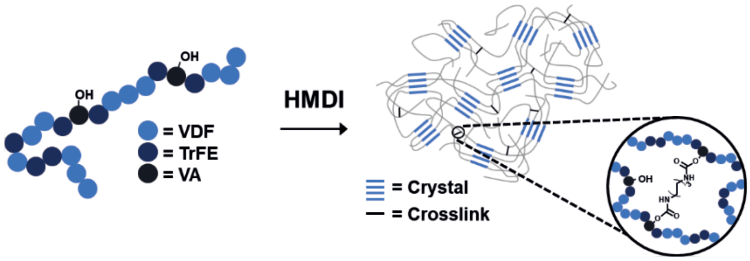

Meereboer et. al., *J. Mater. Chem. A*, **2019**, 7, 2795–2803

Relaxor ferroelectric polymers, having a high energy storage density and efficiency, are rapidly developing for reliable and compact dielectric film capacitors. Until now, they have been based on highly fluorinated monomers lacking functionalities for further modifications, such as good dispersion of nanoparticles or facile crosslinking, to gain enhanced properties. In this work, we study the electroactive properties of a novel class of poly(vinylidene fluoride-*ter*-trifluoroethylene-*ter*-vinyl alcohol) (P(VDF-*ter*-TrFE-*ter*-VA)) terpolymers for capacitive energy storage applications. Additionally, we show that the VA units in these terpolymers can be crosslinked using facile urethane chemistry. It is found that introducing VA in the terpolymer backbone leads to cocrystallization with the fluorinated monomeric constituents. The VA defects promote the formation of TTTG monomer sequences favoring relaxor ferroelectric behavior. Consequently, the Curie transition is strongly reduced compared to P(VDF-*co*-TrFE) analogues. Moreover, chemical crosslinking of P(VDF-*ter*-TrFE-*ter*-VA) terpolymers results in extremely slim hysteresis loops due to the increase in the relative amount of the disordered paraelectric phase and ultrafine crystallites, leading to enhanced charge-discharge efficiencies. Therefore, this new class of relaxor ferroelectric polymers, wherein physical pinning and chemical crosslinking are combined, shows great promise for future advanced applications.

Introduction

Advanced electronic devices and circuits, pulsed power technologies and electric vehicles are among others applications that need high energy density dielectrics for capacitive energy storage.[1–3] Nowadays, by selecting polymers as the material of choice, main requirements such as lightweight nature, low cost, ease of processing, self-healing capability and high breakdown strengths are easily fulfilled. Unfortunately, inherent to commercially available high breakdown strength polymers are low dielectric constants, suppressing the maximum energy densities to be stored inside the dielectrics. For instance, state-of-the-art BOPP shows an energy density of just ~4 J cm^{-3} at an electric field of 600 MV m^{-1}. Therefore, to improve the energy storage in dielectrics, they require both a high dielectric constant (ε) and high breakdown strength, since the stored energy density (U) is proportional to the dielectric constant and the electric field (E) squared as displayed in Equation 6.1, wherein ε_0 is the permittivity in free space.

$$U = \frac{1}{2}\varepsilon\varepsilon_0 E^2 \qquad (6.1)$$

In contrast, poly(vinylidene fluoride) (PVDF) has both a high dielectric constant (~10) and breakdown strength (~600 MV m^{-1}), making it an excellent choice to be used as dielectric material.[4,5] However, an irreversible crystalline phase transformation from the α- to the ferroelectric β-phase at high electric fields results in ferroelectric behavior, which suffers from large hysteresis losses.[6] Accordingly, research efforts focus on tuning the crystal isomorphism, crystallite size and crystalline-amorphous interface of PVDF-based (co)polymers to yield slim hysteresis loops (*i.e.* relaxor or double hysteresis loop (DHL) behavior) while still having large polarizations.[5,7–15]

As such, co- and terpolymerizations of VDF with other fluorinated comonomers, like trifluoroethylene (TrFE), chlorotrifluoroethylene (CTFE) and chlorofluoroethylene (CFE), have been employed to gradually increase the crystal lattice spacing.[16,17] Dependent on the processing conditions, incorporating these comonomers with a lower dipole moment leads to the formation of physical pinning spots, destabilizing the ferroelectric phase and enhancing the dipole reversibility, which results in relaxor ferroelectric behavior. Moreover, in a P(VDF-*ter*-TrFE-*ter*-CTFE) terpolymer, a specific monomer composition leads to a near room temperature Curie transition accompanied with large dielectric constants (ε = 50), rendering these materials suitable for electrocaloric cooling devices as well.[18,19] Interestingly, the Wang group revealed that tacticity in P(VDF-*co*-TrFE) copolymers plays a crucial role in the electroactive behavior.[20] Here, stereochemical changes (from mainly syndiotactic to isotactic sequences) induced by stereospecific TrFE monomers leads to an order-to-disorder evolution in the crystalline phase at >45 mol% TrFE, which results in an increasing amounts 3/1 helices as opposed to the all-trans

planar conformations - changing its behavior from ferroelectric to relaxor ferroelectric behavior.[20] Additionally, after mechanical stretching, bulky hexafluoropropylene (HFP) monomeric constituents are incorporated in the polymer crystals leading to relaxor ferroelectric behavior, which is caused by a break up of large ferroelectric nanodomains into smaller nonpolar regions.[21] P(VDF-*co*-CTFE) copolymers grafted with polystyrene (PS) or poly(alkyl methacrylate) (PAMA) are another means to avert ferroelectric behavior in PVDF.[7,22,23] Here, PS or PAMA side chains segregate to the crystalline-amorphous interface, creating a nonpolar confining layer that effectively destabilize the ferroelectric domains, resulting in DHL behavior. These strategies change the electroactive behavior of PVDF drastically and show increased released energy densities and efficiencies.

Alternative strategies to modify PVDF to render dielectric materials include chemical crosslinking. In this way, small nanocrystals are formed while additionally increasing the dielectric breakdown strength of the material due to an enhancement of the mechanical properties.[24,25] Unfortunately, effective ways to gain control over the crosslinking sites in fluorinated polymers are rare due to the lack of functionalities in the fluorinated backbones. Nevertheless, chemical crosslinking is performed using peroxides and triallyl isocyanurate (TI), diamines or electrobeam irridation.[24,26,27] In particular, the use of peroxides and TI to crosslink P(VDF-*co*-CTFE) results in excellent dielectric performance having high efficiencies and large released energy densities (83% and 17 J cm^{-3} at 400 MV m^{-1}, respectively), showing the great potential of chemically crosslinked PVDF for capacitive energy storage applications.

Recently, we have shown how vinyl alcohol (VA) units can easily be introduced in the PVDF backbone.[28] Due to the small size of the monomeric units, they can be included in the PVDF crystals, increasing the crystal lattice size and act as pinning spots. Moreover, these hydroxyl functionalities, being well distributed over the polymer backbone, can be used to do easy additional chemistries to improve for example nanoobject dispersion, adhesion to interfaces, and crosslinking. In this work, physical pinning and chemical crosslinking are combined to obtain narrow hysteresis loops with high polarization. We demonstrate the synthesis and chemical crosslinking of P(VDF-*ter*-TrFE-*ter*-VA) terpolymers and show its electroactive behavior. In addition, the effect of VA units on the thermal behavior in the terpolymers is investigated, showing how VA units change properties such as the Curie transition temperature. Strong reductions in the Curie transition temperature of the P(VDF-*ter*-TrFE-*ter*-VA) terpolymers are found, while the crosslinked materials display narrow hysteresis loop relaxor ferroelectric behavior, making them highly suitable for capacitive energy storage applications.

Materials and Methods

Experimental

Materials: Benzoyl peroxide was recrystallized prior to use. Vinyl acetate was dried over CaH_2 and distilled under reduced pressure. Vinylidene fluoride (VDF, Synquest Labs, 98%), trifluoroethylene (TrFE, Synquest Labs, 98%), Hexamethylenediisocyanate (HMDI, TCI, 98%) and cyclopentanone (TCI, >99%) were used as received. All solvent are obtained from commercial resources and used without further purification.

Synthesis of P(VDF-ter-TrFE-ter-VAc) terpolymers: A 600 mL Parr (model 4568) high pressure reactor was charged with benzoyl peroxide (150 mg, 0.62 mmol), anhydrous dimethyl carbonate (300 mL), and freshly distilled vinyl acetate (VAc, 1 mL, 10.9 mmol). After the reaction mixture was purged with N_2 for 30 min, TrFE (2.5 bar) and VDF (to 15 bar) were transferred into the reactor at room temperature. The reaction mixture was rapidly heated to 90 °C and allowed to stir at 500 rpm for 30 min. Subsequently, the heating source was removed and the reaction mixture was cooled to room temperature using a water flow. Excess of TrFE and VDF were removed by depressurizing the reaction vessel. The solution was concentrated in vacuo in order to precipitate the copolymer in a water/methanol mixture. Excess of initiator was removed by extensively washing with chloroform. Finally, the copolymer was dried in a vacuum.

Synthesis of P(VDF-ter-TrFE-ter-VA) terpolymers: A general synthetic procedure is described as follows: a round-bottom flask was charged with 1.0 grams of P(VDF-*ter*-TrFE-*ter*-VAc) terpolymers, dioxane (80 mL), and concentrated hydrochloric acid (8 mL). The reaction mixture was stirred over night at 60 °C. The mixture was concentrated in vacuo, after which the copolymer was precipitated by adding a large excess of water. Subsequently, the copolymer was collected *via* filtration followed by extensive washing with water to remove residual side product and hydrochloric acid, yielding 0.8 grams of white P(VDF-*ter*-TrFE-*ter*-VA) terpolymers.

Crosslinking of P(VDF-ter-TrFE-ter-VA) terpolymers: P(VDF-*ter*-TrFE-*ter*-VA) (25 mg, mmol VA) and HMDI (C1, µL, mmol or C2, µL, mmol) were combined in 1.5 mL cyclopentanone and allowed to mix at 80 °C for 30 min. After cooling down to room temperature, the solution was passed through a 0.45 µm PTFE filter into an aluminum pan (ø 3 mm). Pristine P(VDF-*ter*-TrFE-*ter*-VA) terpolymers were after dissolving in cyclopentanone (40 mg in 1.5 mL) directly transferred in an aluminum pan using a 0.45 µm PTFE filter. The aluminum pan was transferred to a heating plate set at 130 °C to induce crosslinking and evaporation of solvent. The next day, the (crosslinked) samples were heated to 160 °C to erase thermal history and subsequently quenched at room temperature. Subsequently, ~10 µm thick free-standing films are obtained *via* a lift-off method in water. All samples were dried overnight under a vacuum.

Characterization

NMR spectroscopy: ^{1}H and ^{19}F NMR (COSY) spectra were recorded on Varian (VXR) spectrometer operating at 400 MHz for the ^{1}H nucleus and 376 MHz for the ^{19}F nucleus. The composition was determined *via* the following method. First, the ratio between VDF and TrFE ($r_{VDF/TrFE}$) was calculated using ^{19}F NMR spectroscopy.[20] The ratio of TrFE and VA was determined using ^{1}H NMR spectroscopy according to the following equation:

$$r_{TrFE/VA} = \frac{\int_{5.10}^{6.00} CH_{TrFE}}{((\int_{4.11}^{5.00} CH_{VA} + OH_{VA})/2)}$$

Consequently, using the ratios $r_{VDF/TrFE}$ and $r_{TrFE/VA}$, the terpolymer composition was obtained.

Fourier Transform Infrared Spectroscopy: The FTIR spectra of the copolymers were recorded on a Bruker Vertex 70 spectrophotometer using 32 scans at a nominal resolution of 4 cm^{-1} using a diamond single reflection attenuated total reflectance (ATR).

Differential scanning calorimetry (DSC): DSC thermograms were recorded on a TA Instruments DSC Q1000. The heating and cooling rate was set to be 10 °C min^{-1}.

Wide-angle X-ray scattering (WAXS): WAXS measurements was performed at beamline BM26B at the European Synchrotron Radiation Facility (ESRF) in Grenoble with a wavelength λ = 0.97 Å. The WAXS pattern was acquired over a time interval of 30 seconds using a Pilatus 300K detector (1472 × 195 pixels of 172 µm × 172 µm placed at a distance of 0.28 m. The scattering vector q is defined as $q = 4\pi/\lambda(\sin\vartheta)$ with 2θ being the scattering angle. Deconvolution of the WAXS profiles was achieved using MATLAB. The experimental profiles were deconvoluted by using the sum of a linear background and pseudo-Voigt peaks describing the scattering from the amorphous and the crystalline phases.

Electrical characterization: D-E and *I-E* loops were obtained using a state-of-the-art aixACCT TF2000E ferroelectric tester where AC electric fields (up to 10 kV) were applied across the polymer films with a triangular waveform at a frequency of 10 Hz. Chromium (5 nm) / gold (100 nm) electrodes with a diameter of 2 mm were deposited on both sides of P(VDF-*co*-VA) copolymer films by vapor deposition. Chromium was used only as adhesion layer. Silicon oil was used to prevent flashovers.

Results and Discussion

The synthesis and crosslinking of P(VDF-*ter*-TrFE-*ter*-VA) terpolymers is outlined in Scheme 6.1. To show the impact of the introduction of VA units in the P(VDF-*ter*-TrFE-*ter*-VA) terpolymers on the thermal and electroactive behavior, we synthesized two different terpolymers having a similar TrFE/VA ratio. P($VDF_{0.78}$-*ter*-$TrFE_{0.17}$-*ter*-$VA_{0.05}$) and P($VDF_{0.53}$-*ter*-$TrFE_{0.37}$-*ter*-$VA_{0.10}$). Because P(VDF-*co*-TrFE) copolymers containing 50 or 80 mol% VDF are on the verge of solely crystallizing in the ferroelectric phase, replacing TrFE units for VA, while having a similar amount of VDF, allows for a good comparison to literature reports.[20,29]

Because the tautomerization equilibrium of vinyl alcohol lies on the acetaldehyde side, P(VDF-*ter*-TrFE-*ter*-VA) was synthesized indirectly using vinyl acetate (VAc) in the terpolymerization reaction.[30] As such, *via* a free radical polymerization, VDF, TrFE and VAc were terpolymerized in dimethyl carbonate (DMC) using benzoyl peroxide (BPO) as initiator. DMC was selected as solvent due to a good trade-off between reaction rate and chain transfer to solvent.[31] It is understood from the literature that terpolymerizations of vinyl monomers, such as 3,3,3-trifluoropropene (TFP), with VDF and TrFE lead to compositional heterogeneity when high conversions are achieved as TFP prefers to homopropagate due to large differences in reactivity ratios.[32] To mitigate concerns regarding compositional heterogeneity, the reaction times are kept short (with minimal pressure drop < 2 bar to prevent large variations in VDF and TrFE concentrations) and the VAc content is kept low to minimize the compositional drift due to the large differences in reactivity ratios between VDF and VAc leading to the preferential consumption of VAc during the polymerization.[28,33,34]

After the polymerization, the presence of unreacted VAc was confirmed by ^{1}H NMR spectroscopy indicating that no P(VDF-*co*-TrFE) copolymers were formed. Subsequently, hydrolysis of the P(VDF-*ter*-TrFE-*ter*-VAc) terpolymers in a dioxane/HCl mixture yielded P(VDF-*ter*-TrFE-*ter*-VA). Noteworthy, acidic conditions were used to hydrolyze the terpolymers to prevent dehydrofluorination reactions.

In Figure 6.1, the ^{1}H NMR spectra demonstrate the complete removal of the acetyl groups by the disappearance corresponding methyl protons located at 2.00 ppm, proving a successful full conversion to the hydroxyl functionalized terpolymers. Additionally, an upfield shift of the methine protons (-C<u>*H*</u>(OH)-) to 4.11-4.60 ppm confirms the formation of hydroxyl groups, which protons are located in between 4.11-5.00 ppm. Moreover, the multiple correlation signals in the ^{1}H NMR correlation spectrum (Figure 6.2) reveal that the methine proton of the vinyl alcohol units correlate with different monomer sequences of both VDF (-C<u>*H*</u>$_2$$CF_2$-, ~2.26 ppm) and TrFE (-C<u>*H*</u>FCF_2-, 5.15, 5.65, 6.3 ppm), indicating the good distribution of VA units in the backbone. Previous work in our group

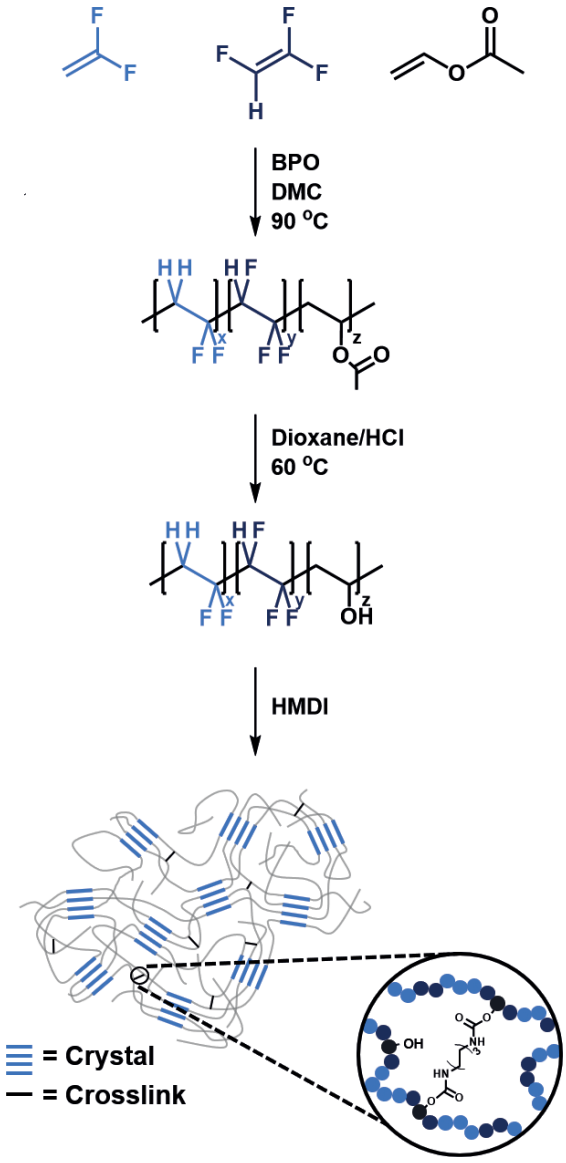

Scheme 6.1: Synthetic approach towards chemically crosslinked P(VDF-*ter*-TrFE-*ter*-VA) terpolymers.

already demonstrated the excellent dispersion of VA units (up to 15 mol%) in P(VDF-*co*-VA) copolymers, where similar reaction conditions were applied.[28]

However, different from those of P(VDF-*co*-VA) copolymers, the ^{1}H NMR spectra (Figure 6.1) of the P(VDF-*ter*-TrFE-*ter*-VA) terpolymers show an additional signal that appears around 4.80 ppm. This is attributed to the –OH protons of VA units adjacent to TrFE units and the signal becomes more pronounced when the TrFE content in the terpolymer composition is increased, highlighting the difference of the microstructure between the two terpolymers used in this study. Here, the fluorine atom TrFE in –CH(OH)C*H*FCF$_2$– causes more deshielding leading to a downfield shift compared to the hydroxyl group of VA next to a VDF unit.[28] Because there is a clear distinction between the VA protons and the –C*H*F– protons corresponding to TrFE (5.10–6.00 ppm), the ratio between TrFE and VA can be easily determined. From the ^{19}F NMR spectra (Figure 6.3), the ratio between VDF and TrFE is obtained, allowing the terpolymer composition to be calculated.

To examine the thermal characteristics of the terpolymers, P(VDF$_{0.78}$-*ter*-TrFE$_{0.17}$-*ter*-VA$_{0.05}$) and P(VDF$_{0.53}$-*ter*-TrFE$_{0.37}$-*ter*-VA$_{0.10}$), we performed differential scanning calorimetry (DSC) measurements. As shown in Figure 6.4, replacing TrFE units for VA in the polymer backbone has a profound influence on the thermal behavior of the terpolymers.[20,35] The crystallization temperature (T_{cr}) of P(VDF$_{0.78}$-*ter*-TrFE$_{0.17}$-*ter*-VA$_{0.05}$) is determined to be 93 °C, while the Curie transition temperature (T_c) dropped to 55 °C, about 25 °C lower than P(VDF-*co*-TrFE) with equal VDF content. Similar behavior is observed in the melting scan. In here, a sharp Curie transition is having a maximum at 79 °C and the polymer is completely molten at 120 °C, both values strongly reduced comparted to P(VDF-*co*-TrFE) with 22 mol% TrFE inside (T_c ~ 100 °C, T_m ~ 148 °C).[35] P(VDF$_{0.53}$-*ter*-TrFE$_{0.37}$-*ter*-VA$_{0.10}$), containing less VDF and a comparable ratio TrFE/VA, demonstrates a similar crystallization temperature as P(VDF$_{0.78}$-*ter*-TrFE$_{0.17}$-*ter*-VA$_{0.05}$), while the Curie

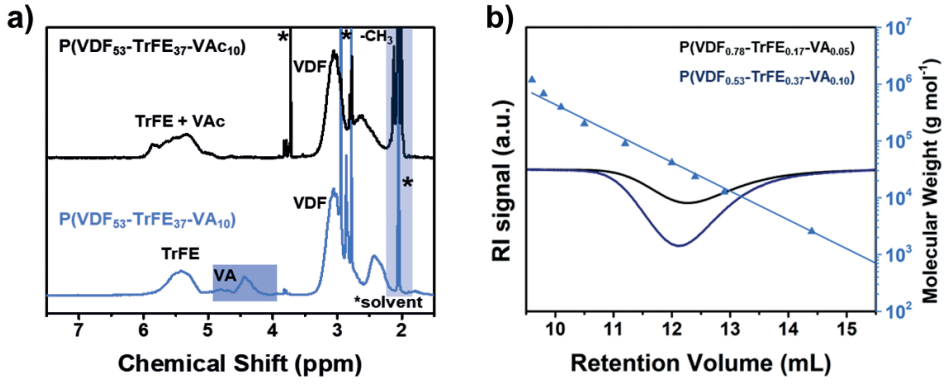

Figure 6.1: (a) ^{1}H NMR spectra of P(VDF$_{0.53}$-*ter*-TrFE$_{0.37}$-*ter*-VAc$_{0.10}$) and P(VDF$_{0.53}$-*ter*-TrFE$_{0.37}$-*ter*-VA$_{0.10}$), showing the successful hydrolysis. (b) GPC traces of the P(VDF-*ter*-TrFE-*ter*-VA) copolymers

transition temperature is lowered to 40 °C. Upon heating, the reverse process involves a Curie transition at 46 °C and the terpolymer is completely molten at 149 °C. The large difference in melting temperature of the terpolymers is analogous to that of P(VDF-*co*-TrFE) copolymers. Here, the T_m takes a minimum value with 90 mol% VDF inside and is shifted to higher values when the VDF or TrFE content is increased, moving towards the T_m of its parent homopolymers.[35] As expected, an increasing TrFE content in the terpolymers lowers the Curie transition temperature. Even though the Curie transition temperature

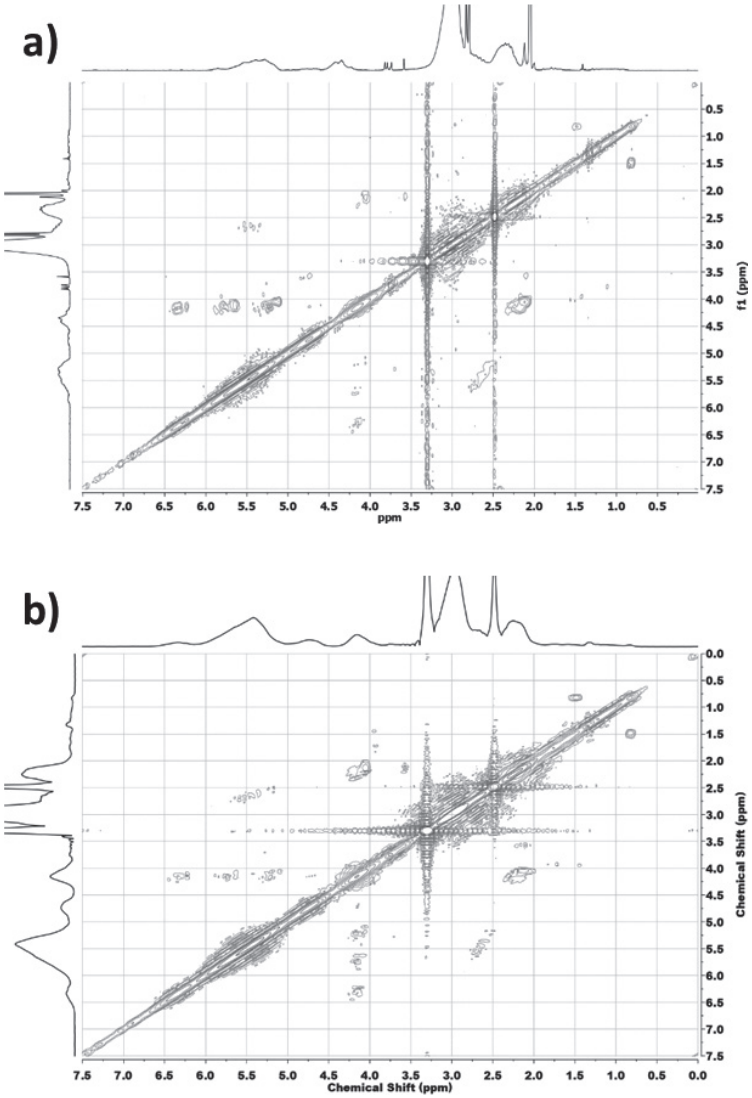

Figure 6.2: ^{1}H NMR COSY spectrum of (a) P(VDF$_{0.78}$-*ter*-TrFE$_{0.17}$-*ter*-VA$_{0.05}$) and (b) P(VDF$_{0.53}$-*ter*-TrFE$_{0.37}$-*ter*-VA$_{0.10}$).

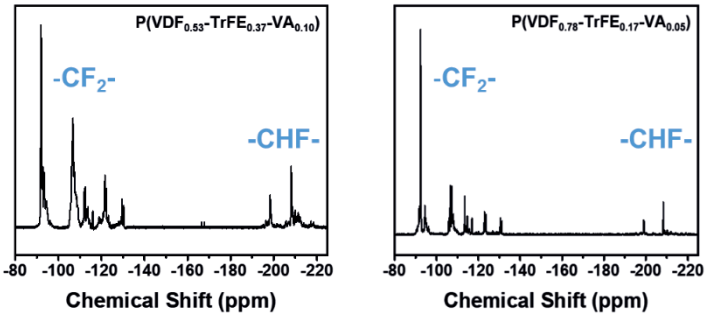

Figure 6.3:[19]F NMR spectrum of the terpolymers.

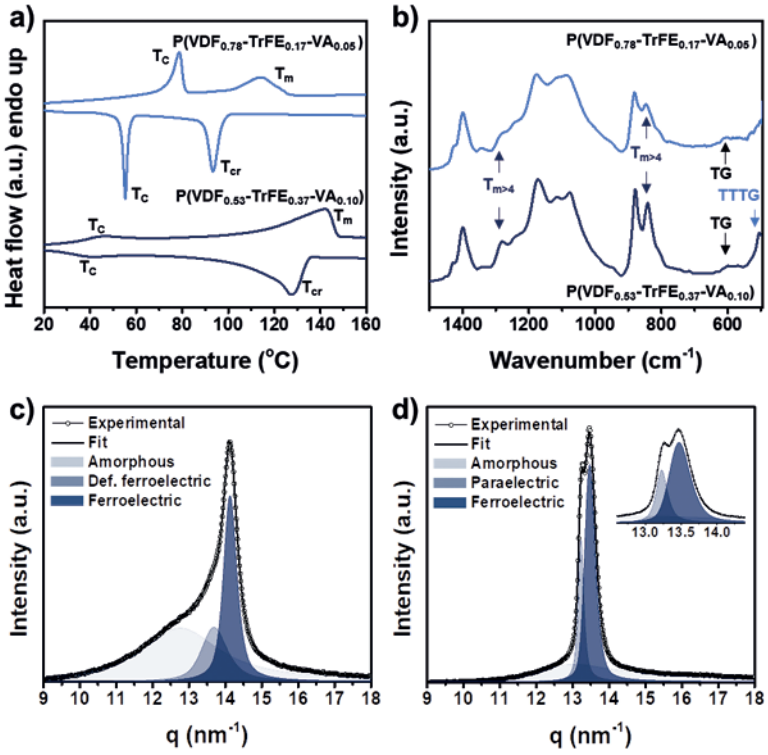

Figure 6.4: (a) DSC thermograms and (b) FTIR spectra of the P(VDF-*ter*-TrFE-*ter*-VA) terpolymers. WAXS profiles of (c) P($VDF_{0.78}$-*ter*-$TrFE_{0.17}$-*ter*-$VA_{0.05}$) and d) P($VDF_{0.53}$-*ter*-$TrFE_{0.37}$-*ter*-$VA_{0.10}$).

in P(VDF-*co*-TrFE) copolymers can be slightly varied by tuning the processing conditions or polymerization method, the terpolymers show a T_c much lower than obtained for P(VDF-*co*-TrFE) having a similar VDF content.[36–38] This result is quite remarkable, since it is generally believed that monomers having a larger size (TrFE > VA) facilitate in reducing the Curie transition temperature.[8] In comparison, P(VDF-*ter*-TrFE-*ter*-CTFE) terpolymers, wherein CTFE also cocrystallizes with VDF and TrFE regardless of the melt crystallization

conditions, show also a reduction in Curie transition when TrFE units are replaced by CTFE.[19,39] A third monomer introduced into the polymer backbone acts as a defect allowing an increase in the crystal lattice spacing and more $TTTG^+TTTG^-$ conformations (T = *trans* and G = *gauche*), as opposed to the densely packed all-trans conformation in ferroelectric P(VDF-*co*-TrFE). This increase in the disordered paraelectric phase content and the increased interchain distance in the crystals lowers the required energy barrier for the Curie transition, leading to a room temperature phase transition for P($VDF_{0.79}$-*ter*-$TrFE_{0.07}$-*ter*-$CTFE_{0.14}$).

To further elucidate the effect of VA incorporation in the terpolymer backbone on the crystallization behavior, wide-angle X-ray scattering (WAXS) and Fourier transform infrared spectroscopy (FTIR) are performed (Figure 6.4). Absorbance peaks belonging to the specific monomer conformations are located around 507 (TTTG), 614 (TG), 840 ($T_{m>4}$) and 1280 cm^{-1} ($T_{m>4}$) in the FTIR spectra. [20,40] The P($VDF_{0.53}$-*ter*-$TrFE_{0.37}$-*ter*-$VA_{0.10}$) shows, next to the $T_{m>4}$ conformations, the characteristic TTTG and TG absorption band at 506 cm^{-1} and 612 cm^{-1}. Even though the absorption bands associated with the TTTG are absent in P($VDF_{0.78}$-*ter*-$TrFE_{0.17}$-*ter*-$VA_{0.05}$), the peaks corresponding to the $T_{m>4}$ conformations are present albeit less intense just as the TG absorption bands. Interestingly, a recent study using ^{19}F NMR spectroscopy and computational data showed that isotactic TrFE-TrFE segments preferentially crystallize in an 3/1 helical conformation having TTTG conformations.[20,41] Indeed, comparing the ^{19}F NMR spectra of the VA-based terpolymers used in this study, P($VDF_{0.53}$-*ter*-$TrFE_{0.37}$-*ter*-$VA_{0.10}$) shows a large increase in the signals in the region around -212 ppm confirming isotactic TrFE-TrFE linkages.

As expected, P($VDF_{0.78}$-*ter*-$TrFE_{0.17}$-*ter*-$VA_{0.05}$) is in the ferroelectric phase at room temperature, as evidenced by the concomitant (110/200) WAXS peaks located at 14.15 nm^{-1} (Figure 6.4c). Moreover, peak deconvolution reveals an additional crystalline phase at 13.7 nm^{-1}, which is recognized as a ferroelectric phase having gauche defects.[42,43] In contrast, as DSC and FTIR spectroscopy already suggested, P($VDF_{0.53}$-*ter*-$TrFE_{0.37}$-*ter*-$VA_{0.10}$) shows a completely different crystallization behavior. In the WAXS profile depicted in Figure 6.4d, the coexistence of two crystalline phases characterized by two different peaks located at 13.24 and 13.48 nm^{-1} is revealed. Next to the characteristic ferroelectric phase peak located at 13.48 nm^{-1}, a second peak located at 13.24 nm^{-1} is present and it is associated with the existence of a disordered paraelectric structure, in agreement with many literature reports.[20,44–47] The large shift to lower q-values in P($VDF_{0.53}$-*ter*-$TrFE_{0.37}$-*ter*-$VA_{0.10}$) is attributed to the inclusion of more TrFE units increasing the spacing between the reflective planes. Additionally, since the 100% melting enthalpies are unknown, WAXS is used to determine the crystallinity of the terpolymers. Interestingly, an increasing trend is observed upon higher TrFE content in the fluorinated VA-based polymers samples. From a previous study, P(VDF-*co*-VA) shows a degree of crystallinity of 38%, whereas the crystallinity in P($VDF_{0.78}$-*ter*-$TrFE_{0.17}$-*ter*-$VA_{0.05}$) and P($VDF_{0.53}$-*ter*-$TrFE_{0.37}$-*ter*-$VA_{0.10}$) is

calculated to be 48% and 63%, respectively.[28] It is believed that the increasing size of TrFE monomers overcomes structural imperfections induced by VA units allowing more VA to be included in the crystal lattices. Noteworthily, in the VA-based terpolymers, similar or higher degree of crystallinities are obtained as compared to P($VDF_{0.53}$-*co*-$TrFE_{0.47}$), P(VDF-*ter*-TrFE-*ter*-CTFE) and P(VDF-*ter*-TrFE-*ter*-CFE) that demonstrate appealing electroactive behavior for dielectric applications.[8,20,39]

One major advantage of the P(VDF-*ter*-TrFE-*ter*-VA) terpolymers is having easily accessible hydroxyl functional groups that allows facile modifications. Using these hydroxyl functionalities for crosslinking offers an opportunity to break up large ferroelectric crystalline domains so that slim hysteresis loops can be obtained, while still having high polarizations.[5,7,8] Due to its high degree of crystallinity and crystalline phases beneficial for energy storage applications, it was decided to crosslink P($VDF_{0.53}$-*ter*-$TrFE_{0.37}$-*ter*-$VA_{0.10}$) using hexamethylene diisocyanate (HMDI) with 0.1-, 0.25- and 0.5-fold excess of isocyanate to hydroxyl groups. The crosslinked fluorinated networks are designated according to their isocyanate excess used, namely P($VDF_{0.53}$-*ter*-$TrFE_{0.37}$-*ter*-$VA_{0.10}$)-0.1x, P($VDF_{0.53}$-*ter*-$TrFE_{0.37}$-*ter*-$VA_{0.10}$)-0.25x and P($VDF_{0.53}$-*ter*-$TrFE_{0.37}$-*ter*-$VA_{0.10}$)-0.5x.

As expected, the crosslinked fluoropolymers are insoluble in common organic solvents, such as dimethylformamide (DMF), proving its crosslinked nature (DMF is a good solvent for P(VDF-*ter*-TrFE-*ter*-VA) terpolymers). In addition, the FTIR spectra, shown in Figure 6.5a, demonstrate the formation of urethane bonds as indicated by the appearance of the carbamate absorption band at 1525 cm^{-1} and the carbonyl stretching at 1704 cm^{-1}. Moreover, no grafting of the P($VDF_{0.53}$-*ter*-$TrFE_{0.37}$-*ter*-$VA_{0.10}$) terpolymers occurred, which is demonstrated by the absence of the asymmetric stretch of isocyanate groups expected to be at around 2277 cm^{-1}.[38]

The crystalline phases of the crosslinked terpolymers were analyzed using FTIR spectroscopy and WAXS as demonstrated in Figure 6.5. Indeed, the crystallization behavior is drastically changed upon crosslinking. The crystallinity of crosslinked P($VDF_{0.53}$-*ter*-$TrFE_{0.37}$-*ter*-$VA_{0.10}$) terpolymers reduces with increasing use of crosslinking agent as shown in Table 6.1. Nevertheless, peak deconvolution of the WAXS profiles reveals that the fraction of paraelectric phase in the crosslinked samples progressively increases when the amount of crosslinking agent is increased. This is supported by analysis of the FTIR spectra, where the absorption band at 506 cm^{-1} corresponding to the TTTG conformation becomes more pronounced, while the bands showing the $T_{m>4}$ conformations reduce in intensity. Moreover, crosslinking reduces the crystallite size of the paraelectric crystals in the terpolymers from 34.9 nm for pristine P($VDF_{0.53}$-*ter*-$TrFE_{0.37}$-*ter*-$VA_{0.10}$) to just 15.0 nm for P($VDF_{0.53}$-*ter*-$TrFE_{0.37}$-*ter*-$VA_{0.10}$) crosslinked with 0.5-fold excess of HMDI. Due to the well-distributed crosslinking sites in the fluorinated networks, only small disordered paraelectric crystals are formed, separated by chemical crosslinks. This reduction in the average disordered paraelectric crystallite size is well evidenced by the increase of

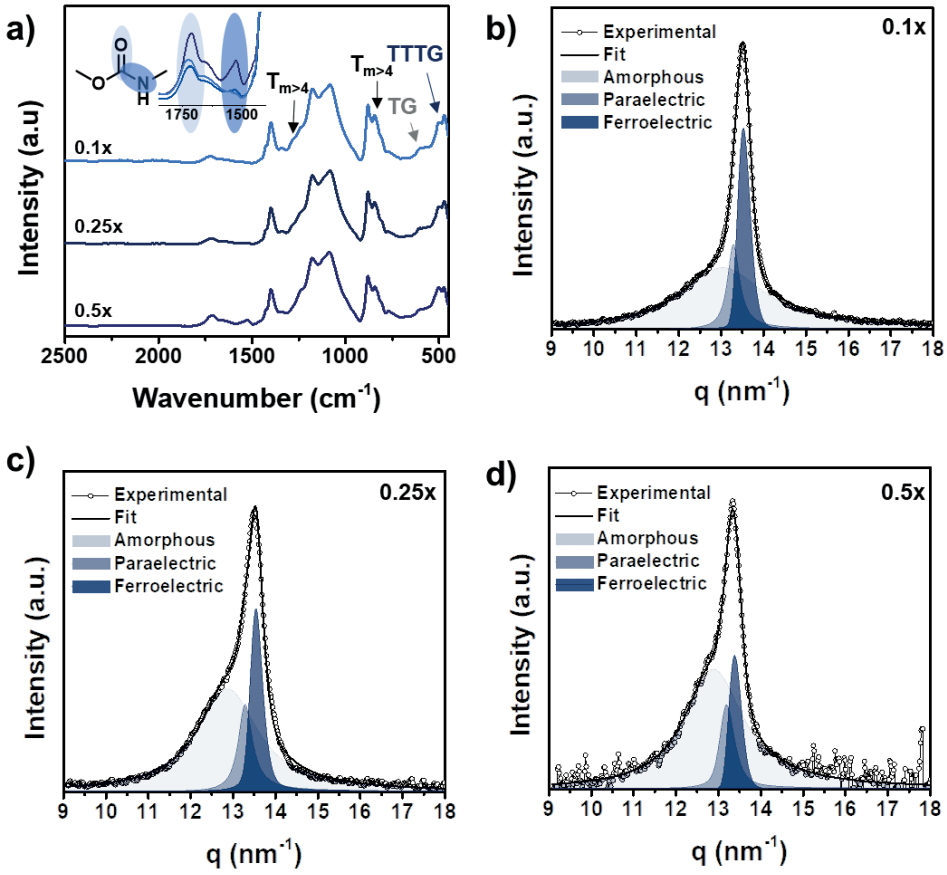

Figure 6.5: (a) FTIR spectra of the crosslinked P(VDF$_{0.53}$-*ter*-TrFE$_{0.37}$-*ter*-VA$_{0.10}$) terpolymers. (b) WAXS profile of P(VDF$_{0.53}$-*ter*-TrFE$_{0.37}$-*ter*-VA$_{0.10}$)-0.1x. (c) Schematic representation of the crosslinked terpolymers. (d) WAXS profile of P(VDF$_{0.53}$-*ter*-TrFE$_{0.37}$-*ter*-VA$_{0.10}$)-0.25x. (e) *D-E* loop of P(VDF$_{0.53}$-*ter*-TrFE$_{0.37}$-*ter*-VA$_{0.10}$) and the crosslinked terpolymers. (f) WAXS profile of P(VDF$_{0.53}$-*ter*-TrFE$_{0.37}$-*ter*-VA$_{0.10}$)-0.5x.

Table 6.1: Crystallization characteristics of the polymers used in this study.

Polymer	X_c [a] (%)	F_p [b]	F_f [c]	FWHM$_p$ (nm^{-1})[d]	FWHM$_f$ (nm^{-1})[e]	d_p (nm)[f]	d_f (nm)[g]
P(VDF$_{0.53}$-TrFE$_{0.37}$-VA$_{0.10}$)	63	0.30	0.70	0.18	0.35	34.9	18.0
P(VDF$_{0.53}$-TrFE$_{0.37}$-VA$_{0.10}$)-0.1x	38	0.37	0.63	0.34	0.35	18.5	18.0
P(VDF$_{0.53}$-TrFE$_{0.37}$-VA$_{0.10}$)-0.25x	34	0.41	0.59	0.40	0.35	15.7	18.0
P(VDF$_{0.53}$-TrFE$_{0.37}$-VA$_{0.10}$)-0.5x	26	0.48	0.52	0.42	0.35	15.0	18.0

[a]Degree of crystallinity calculated from the WAXS profiles. [b]Fraction of paraelectric phase. [c]Fraction of ferroelectric phase.[d]Full width half maximum of the [d]paraelectric and [e]ferroelectric phase. Crystallite size calculated using the Scherrer equation of the [f]paraelectric and [g]ferroelectric phase.

the peak width with increasing crosslinking as determined from WAXS (Table). In the literature, a similar crystal size reduction is also observed in crosslinking of P(VDF-*co*-CTFE), while other crosslinking methods, such as electrobeam irradiation, offer poor control over the crosslinking site, resulting in a large distribution of crystallite sizes.[24,49]

To compare the electroactive behavior of the (crosslinked) terpolymers, displacement-electric field (*D*-*E*) measurements were performed by applying an electric field up to 250 MV m^{-1} in a triangular wave form at a frequency of 10 Hz, measuring the polarization as the integral of the resulting current. At lower electric fields (<80 MV m^{-1}), the (crosslinked) terpolymers show linear dielectric behavior. Consequently, by calculating the stored energy density and using Advanced electronic devices and circuits, pulsed power technologies and electric vehicles are among others applications that need high energy density dielectrics for capacitive energy storage.[1–3] Nowadays, by selecting polymers as the material of choice, main requirements such as lightweight nature, low cost, ease of processing, self-healing capability and high breakdown strengths are easily fulfilled. Unfortunately, inherent to commercially available high breakdown strength polymers are low dielectric constants, suppressing the maximum energy densities to be stored inside the dielectrics. For instance, state-of-the-art BOPP shows an energy density of just ~4 J cm^{-3} at an electric field of 600 MV m^{-1}. Therefore, to improve the energy storage in dielectrics, they require both a high dielectric constant (ε) and high breakdown strength, since the stored energy density (U) is proportional to the dielectric constant and the electric field (E) squared as displayed in Equation 6.1, the apparent dielectric constant can be derived.[50,51] It is found that P($VDF_{0.78}$-*ter*-$TrFE_{0.17}$-*ter*-$VA_{0.05}$) and P($VDF_{0.53}$-*ter*-$TrFE_{0.37}$-*ter*-$VA_{0.10}$) show an apparent dielectric constant (ε_{app}) of 20 and 45, respectively, while it is progressively reducing for the crosslinked samples due to the lower degree of crystallinity (Table 6.1). At higher electric fields (250 MV m^{-1}), the ferroelectric dipoles align in P($VDF_{0.78}$-*ter*-$TrFE_{0.17}$-*ter*-$VA_{0.05}$) leading to a polarization of 7.13 µC cm^{-2} and a remanent polarization of 3.10 µC cm^{-2} (Figure 6.6a). The relatively low remanent polarization of P($VDF_{0.78}$-*ter*-$TrFE_{0.17}$-*ter*-$VA_{0.05}$) compared to ferroelectric P(VDF-co-TrFE) copolymers can be ascribed to the formation of physical pinning spots enhancing the dipole reversibility.[5,8,28] In Figure 6.6b, the *D*-*E* loops of P($VDF_{0.53}$-*ter*-$TrFE_{0.37}$-*ter*-$VA_{0.10}$) and the fluorinated networks are depicted at similar electric fields. Here, relaxor ferroelectric behavior is observed in all samples. Due to VA pinning spots in the nanocrystals and the mixture of disordered paraelectric and ferroelectric phases, P($VDF_{0.53}$-*ter*-$TrFE_{0.37}$-*ter*-$VA_{0.10}$) demonstrates a low remanent polarization of 1.01 µC cm^{-2} and a maximum polarization of 5.52 µC cm^{-2} at 250 MV m^{-1}. This relaxor ferroelectric behavior shows great similarity with results obtained for other relaxor ferroelectric terpolymers.[5,8,20,39] For example, comparable to P(VDF-*ter*-TrFE-*ter*-CFE), P($VDF_{0.53}$-*ter*-$TrFE_{0.37}$-*ter*-$VA_{0.10}$) demonstrates a charge-discharge efficiency of 65% at 150 MV m^{-1}.[52] Unfortunately, currently available relaxor ferroelectric terpolymers suffer from large ferroelectric losses at higher fields. To mitigate these concerns and to

consequently enhance the charge-discharge efficiencies, while maintaining the large discharge energy densities, ferroelectric crystals are required to be well isolated.[5,15] The crosslinking method of relaxor ferroelectric polymers introduced in this work appears to be very promising. Even though the reduction in crystallinity and increase in the amount of crystals in the disordered paraelectric phase lower the maximum polarization of the crosslinked fluorinated terpolymers, the remanent polarization is also reduced significantly due to better isolation of ferroelectric domains by chemical crosslinking.[5] As such, the P(VDF$_{0.53}$-*ter*-TrFE$_{0.37}$-*ter*-VA$_{0.10}$)-0.5x shows a maximum polarization of 3.45 µC cm^{-2} and a remanent polarization as low as 0.15 µC cm^{-2} at 260 MV m^{-1}, respectively (Figure 6.6 and Table 6.2). This leads to increased charge-discharge efficiencies as clearly visualized in Figure 6.7. For example, at 150 MV m^{-1}, P(VDF$_{0.53}$-*ter*-TrFE$_{0.37}$-*ter*-VA$_{0.10}$) shows an efficiency of 63%, while this increased to 82% for P(VDF$_{0.53}$-*ter*-TrFE$_{0.37}$-*ter*-VA$_{0.10}$)-0.25x, while both have a discharge energy density of 2 J cm^{-3}. Because these materials show great promise for capacitive energy storage applications, future work should be devoted to exploring the full potential of P(VDF-*ter*-TrFE-*ter*-VA) terpolymers, including optimization of the composition of the terpolymers, choice of crosslinking agent and to gain better insights into the high filed dielectric loss and failure mechanisms.

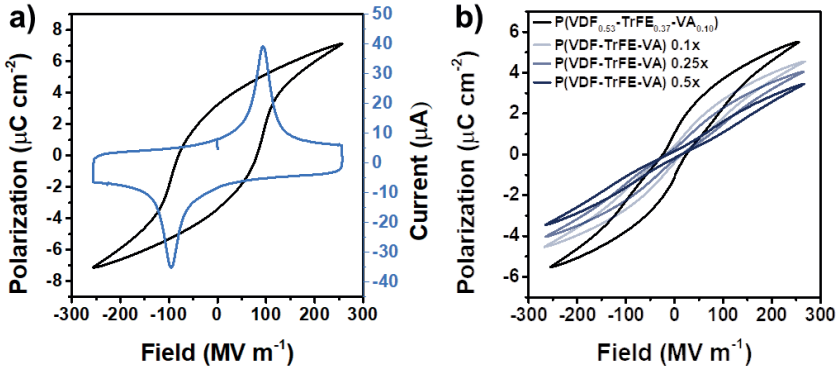

Figure 6.6: *D-E* loops of (a) P(VDF$_{0.78}$-*ter*-TrFE$_{0.17}$-*ter*-VA$_{0.05}$) and (b) P(VDF$_{0.53}$-*ter*-TrFE$_{0.37}$-*ter*-VA$_{0.10}$) and the crosslinked samples.

Table 6.2: Maximum and remanent polarization of the (crosslinked) P(VDF-*ter*-TrFE-*ter*-VA) terpolymers used.

Polymer	P_{max} (µC cm^{-2})	P_{rem} (µC cm^{-2})	Field (MV m^{-1})	ε_{app}
P(VDF$_{0.78}$-TrFE$_{0.17}$-VA$_{0.05}$)	7.13	3.10	250	20.0
P(VDF$_{0.53}$-TrFE$_{0.37}$-VA$_{0.10}$)	5.52	1.01	250	45.3
P(VDF$_{0.53}$-TrFE$_{0.37}$-VA$_{0.10}$)-0.1x	4.54	0.37	260	30.6
P(VDF$_{0.53}$-TrFE$_{0.37}$-VA$_{0.10}$)-0.25x	4.05	0.25	260	20.7
P(VDF$_{0.53}$-TrFE$_{0.37}$-VA$_{0.10}$)-0.5x	3.45	0.15	260	16.4

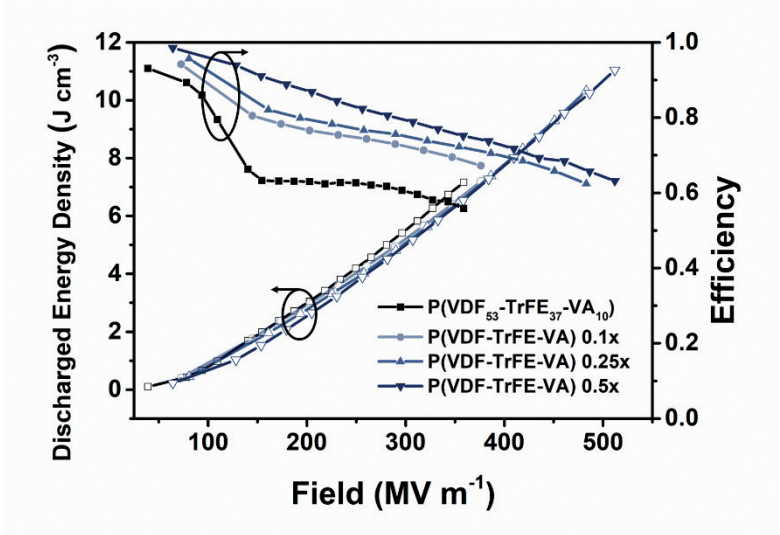

Figure 6.7: The discharged energy densities and charge-discharge efficiencies of P($VDF_{0.53}$-*ter*-$TrFE_{0.37}$-*ter*-$VA_{0.10}$) and the crosslinked terpolymers.

Conclusions

In this chapter, the synthesis and crosslinking of a novel class of P(VDF-*ter*-TrFE-*ter*-VA) terpolymers were demonstrated. The introduction of VA units in the terpolymer backbone drastically changed its crystallization behavior and leads to a reduction of the Curie transition temperature compared to P(VDF-*co*-TrFE) copolymer analogues. The P($VDF_{0.78}$-*ter*-$TrFE_{0.17}$-*ter*-$VA_{0.05}$) terpolymer having a relatively low content of TrFE and VA crystallizes in the ferroelectric phase and demonstrates ferroelectric behavior. In contrast, pristine P($VDF_{0.53}$-*ter*-$TrFE_{0.37}$-*ter*-$VA_{0.10}$) crystallizes in a mixture of the ferroelectric and paraelectric phases resulting in narrow hysteresis behavior with a maximum and remanent polarization of 5.52 µC cm^{-2} and 1.01 µC cm^{-2}, respectively. In addition, chemically crosslinking of P($VDF_{0.53}$-*ter*-$TrFE_{0.37}$-*ter*-$VA_{0.10}$) terpolymers using urethane chemistry promotes the crystallization in the paraelectric phase and the formation of small nanocrystals giving ultra slim hysteresis loops with remanent polarizations as low as 0.15 µC cm^{-2}. The low remanent polarization leads to increased efficiencies for the terpolymers due to a reduction of ferroelectric loss, while maintaining similar discharged energy densities. Since crosslinking relaxor ferroelectric terpolymers show great promise for capacitive energy storage applications, especially due to the large increase in efficiencies, future work should be devoted to exploring the full potential of P(VDF-*ter*-TrFE-*ter*-VA) terpolymers, including optimization of the composition and gain insights in the dielectric loss and failure mechanisms.

References

(1) Bluhm, H. *Pulsed Power Systems: Principles and Applications*; Springer-Verlag: Berlin Heidelberg, **2006**.

(2) Husain, I. Electric and Hybrid Vehicles: Design Fundamentals, Second Edition, 2 edition.; CRC Press: Boca Raton, FL, **2010**.

(3) Teodorescu, R.; Liserre, M.; Rodríguez, P. *Grid Converters for Photovoltaic and Wind Power Systems*; Wiley-Blackwell, **2010**. https://doi.org/10.1002/9780470667057.ch9.

(4) Lovinger, A. J. Ferroelectric Polymers. *Science* **1983**, *220* (4602), 1115–1121. https://doi.org/10.1126/science.220.4602.1115.

(5) Zhu, L.; Wang, Q. Novel Ferroelectric Polymers for High Energy Density and Low Loss Dielectrics. *Macromolecules* **2012**, *45* (7), 2937–2954. https://doi.org/10.1021/ma2024057.

(6) Li, W.; Meng, Q.; Zheng, Y.; Zhang, Z.; Xia, W.; Xu, Z. Electric Energy Storage Properties of Poly(Vinylidene Fluoride). *Appl. Phys. Lett.* **2010**, *96* (19), 192905. https://doi.org/10.1063/1.3428656.

(7) Guan, F.; Yang, L.; Wang, J.; Guan, B.; Han, K.; Wang, Q.; Zhu, L. Confined Ferroelectric Properties in Poly(Vinylidene Fluoride-Co-Chlorotrifluoroethylene)-Graft-Polystyrene Graft Copolymers for Electric Energy Storage Applications. *Advanced Functional Materials* **2011**, *21* (16), 3176–3188. https://doi.org/10.1002/adfm.201002015.

(8) Yang, L.; Li, X.; Allahyarov, E.; Taylor, P. L.; Zhang, Q. M.; Zhu, L. Novel Polymer Ferroelectric Behavior via Crystal Isomorphism and the Nanoconfinement Effect. *Polymer* **2013**, *54* (7), 1709–1728. https://doi.org/10.1016/j.polymer.2013.01.035.

(9) Meereboer, N. L.; Terzić, I.; Saidi, S.; Hermida Merino, D.; Loos, K. Nanoconfinement-Induced β-Phase Formation Inside Poly(Vinylidene Fluoride)-Based Block Copolymers. *ACS Macro Lett.* **2018**, 863–867. https://doi.org/10.1021/acsmacrolett.8b00418.

(10) Terzic, I.; Meereboer, N. L.; Loos, K. CuAAC Click Chemistry: A Versatile Approach towards PVDF-Based Block Copolymers. *Polym. Chem.* **2018**, *9* (27), 3714–3720. https://doi.org/10.1039/C8PY00742J.

(11) Voet, V. S. D.; Brinke, G. ten; Loos, K. Well-Defined Copolymers Based on Poly(Vinylidene Fluoride): From Preparation and Phase Separation to Application. *Journal of Polymer Science Part A: Polymer Chemistry* **2014**, *52* (20), 2861–2877. https://doi.org/10.1002/pola.27340.

(12) Voet, V. S. D.; Ekenstein, G. O. R. A. van; Meereboer, N. L.; Hofman, A. H.; Brinke, G. ten; Loos, K. Double-Crystalline PLLA-b-PVDF-b-PLLA Triblock Copolymers: Preparation and Crystallization. *Polym. Chem.* **2014**, *5* (7), 2219–2230. https://doi.org/10.1039/C3PY01560B.

(13) Voet, V. S. D.; Tichelaar, M.; Tanase, S.; Mittelmeijer-Hazeleger, M. C.; Brinke, G. ten; Loos, K. Poly(Vinylidene Fluoride)/Nickel Nanocomposites from Semicrystalline Block Copolymer Precursors. *Nanoscale* **2012**, *5* (1), 184–192. https://doi.org/10.1039/C2NR32990E.

(14) Soulestin, T.; Ladmiral, V.; Dos Santos, F. D.; Améduri, B. Vinylidene Fluoride- and Trifluoroethylene-Containing Fluorinated Electroactive Copolymers. How Does Chemistry Impact Properties? *Progress in Polymer Science* **2017**, *72*, 16–60. https://doi.org/10.1016/j.progpolymsci.2017.04.004.

(15) Terzic, I.; Meereboer, N. L.; Acuautla, M.; Portale, G.; Loos, K. Electroactive Materials with Tunable Response Based on Block Copolymer Self-Assembly. *Nature Communications* **2019**, *10* (1), 601. https://doi.org/10.1038/s41467-019-08436-2.

(16) Hui-Min Bao; Jiao-Fan Song; Juan Zhang; Qun-Dong Shen, * and; Yang, C.-Z.; Zhang, Q. M. Phase Transitions and Ferroelectric Relaxor Behavior in P(VDF−TrFE−CFE) Terpolymers. *Macromolecules*, **2007**, *40* (7), 2371–2379 https://doi.org/10.1021/ma062800l.

(17) Xu, H.; Cheng, Z.-Y.; Olson, D.; Mai, T.; Zhang, Q. M.; Kavarnos, G. Ferroelectric and Electromechanical Properties of Poly(Vinylidene-Fluoride–Trifluoroethylene–Chlorotrifluoroethylene) Terpolymer. *Appl. Phys. Lett.* **2001**, *78* (16), 2360–2362. https://doi.org/10.1063/1.1358847.

(18) Neese, B.; Chu, B.; Lu, S.-G.; Wang, Y.; Furman, E.; Zhang, Q. M. Large Electrocaloric Effect in Ferroelectric Polymers Near Room Temperature. *Science* **2008**, *321* (5890), 821–823. https://doi.org/10.1126/science.1159655.

(19) Lu, Y.; Claude, J.; Neese, B.; Zhang, Q.; Wang, Q. A Modular Approach to Ferroelectric Polymers with Chemically Tunable Curie Temperatures and Dielectric Constants. *J. Am. Chem. Soc.* **2006**, *128* (25), 8120–8121. https://doi.org/10.1021/ja062306x.

(20) Liu, Y.; Aziguli, H.; Zhang, B.; Xu, W.; Lu, W.; Bernholc, J.; Wang, Q. Ferroelectric Polymers Exhibiting Behaviour Reminiscent of a Morphotropic Phase Boundary. *Nature* **2018**, *562* (7725), 96–100. https://doi.org/10.1038/s41586-018-0550-z.

(21) Xu, H.; Shen, D.; Zhang, Q. Structural and Ferroelectric Response in Vinylidene Fluoride/Trifluoroethylene/Hexafluoropropylene Terpolymers. *Polymer* **2007**, *48* (7), 2124–2129. https://doi.org/10.1016/j.polymer.2007.02.035.

(22) Li, J.; Gong, H.; Yang, Q.; Xie, Y.; Yang, L.; Zhang, Z. Linear-like Dielectric Behavior and Low Energy Loss Achieved in Poly(Ethyl Methacrylate) Modified Poly(Vinylidene-Co-Trifluoroethylene). *Appl. Phys. Lett.* **2014**, *104* (26), 263901. https://doi.org/10.1063/1.4886391.

(23) Li, J.; Hu, X.; Gao, G.; Ding, S.; Li, H.; Yang, L.; Zhang, Z. Tuning Phase Transition and Ferroelectric Properties of Poly(Vinylidene Fluoride-Co-Trifluoroethylene) via Grafting with Desired Poly(Methacrylic Ester)s as Side Chains. *J. Mater. Chem. C* **2013**, *1* (6), 1111–1121. https://doi.org/10.1039/C2TC00431C.

(24) Khanchaitit, P.; Han, K.; Gadinski, M. R.; Li, Q.; Wang, Q. Ferroelectric Polymer Networks with High Energy Density and Improved Discharged Efficiency for Dielectric Energy Storage. *Nature Communications* **2013**, *4*, 2845. https://doi.org/10.1038/ncomms3845.

(25) Tan, S.; Li, J.; Gao, G.; Li, H.; Zhang, Z. Synthesis of Fluoropolymer Containing Tunable Unsaturation by a Controlled Dehydrochlorination of P(VDF-Co-CTFE) and Its Curing for High Performance Rubber Applications. *J. Mater. Chem.* **2012**, *22* (35), 18496–18504. https://doi.org/10.1039/C2JM33133K.

(26) Zhang, Q. M.; Bharti, V.; Zhao, X. Giant Electrostriction and Relaxor Ferroelectric Behavior in Electron-Irradiated Poly(Vinylidene Fluoride-Trifluoroethylene) Copolymer. *Science* **1998**, *280* (5372), 2101–2104. https://doi.org/10.1126/science.280.5372.2101.

(27) Shin, Y. J.; Kim, R. H.; Jung, H. J.; Kang, S. J.; Park, Y. J.; Bae, I.; Park, C. Compression of Cross-Linked Poly(Vinylidene Fluoride-Co-Trifluoro Ethylene) Films for Facile Ferroelectric Polarization. *ACS Appl. Mater. Interfaces* **2011**, *3* (12), 4736–4743. https://doi.org/10.1021/am201202w.

(28) Meereboer, N. L.; Terzić, I.; van der Steeg, P.; Acuautla, M.; Voet, V. S. D.; Loos, K. Electroactive Behavior on Demand in Poly(Vinylidene Fluoride-Co-Vinyl Alcohol) Copolymers. *Materials Today Energy* **2019**, *11*, 83–88. https://doi.org/10.1016/j.mtener.2018.10.019.

(29) Furukawa, T. Structure and Functional Properties of Ferroelectric Polymers. *Advances in Colloid and Interface Science* **1997**, *71–72*, 183–208. https://doi.org/10.1016/S0001-8686(97)90017-8.

(30) Hallensleben, M. L. Polyvinyl Compounds, Others. In *Ullmann's Encyclopedia of Industrial Chemistry*; American Cancer Society, **2000**. https://doi.org/10.1002/14356007.a21_743.

(31) Asandei, A. D.; Adebolu, O. I.; Simpson, C. P. Mild-Temperature Mn2(CO)10-Photomediated Controlled Radical Polymerization of Vinylidene Fluoride and Synthesis of Well-Defined Poly(Vinylidene Fluoride) Block Copolymers. *J. Am. Chem. Soc.* **2012**, *134* (14), 6080–6083. https://doi.org/10.1021/ja300178r.

(32) Soulestin, T.; Ladmiral, V.; Lannuzel, T.; Domingues Dos Santos, F.; Ameduri, B. Importance of Microstructure Control for Designing New Electroactive Terpolymers Based on Vinylidene Fluoride and Trifluoroethylene. *Macromolecules* **2015**, *48* (21), 7861–7871. https://doi.org/10.1021/acs.macromol.5b01964.

(33) Brandrup, J.; Immergut, E. H.; Grulke, E. A. *Polymer Handbook, 4th Edition*; Wiley, **2004**.

(34) Panchalingam, V.; Reynolds, J. R. New Vinylidene Fluoride Copolymers: Poly(Vinyl Acetate-co-vinylidene Fluoride). *Journal of Polymer Science Part C: Polymer Letters* **1989**, *27* (6), 201–208. https://doi.org/10.1002/pol.1989.140270605.

(35) Yagi, T.; Tatemoto, M.; Sako, J. Transition Behavior and Dielectric Properties in Trifluoroethylene and Vinylidene Fluoride Copolymers. *Polymer Journal* **1980**, *12* (4), 209–223. https://doi.org/10.1295/polymj.12.209.

(36) Gregorio, R.; Botta, M. M. Effect of Crystallization Temperature on the Phase Transitions of P(VDF/TrFE) Copolymers. *Journal of Polymer Science Part B: Polymer Physics* **1998**, *36* (3), 403–414. https://doi.org/10.1002/(SICI)1099-0488(199802)36:3<403::AID-POLB2>3.0.CO;2-S.

(37) Kim, K. J.; Kim, G. B.; Vanlencia, C. L.; Rabolt, J. F. Curie Transition, Ferroelectric Crystal Structure, and Ferroelectricity of a VDF/TrFE(75/25) Copolymer 1. The Effect of the Consecutive Annealing in the Ferroelectric State on Curie Transition and Ferroelectric Crystal Structure. *Journal of Polymer Science Part B: Polymer Physics* **1994**, *32* (15), 2435–2444. https://doi.org/10.1002/polb.1994.090321501.

(38) Zhang, Z.; Meng, Q.; Chung, T. C. M. Energy Storage Study of Ferroelectric Poly(Vinylidene Fluoride-Trifluoroethylene-Chlorotrifluoroethylene) Terpolymers. *Polymer* **2009**, *50* (2), 707–715. https://doi.org/10.1016/j.polymer.2008.11.005.

(39) Gadinski, M. R.; Li, Q.; Zhang, G.; Zhang, X.; Wang, Q. Understanding of Relaxor Ferroelectric Behavior of Poly(Vinylidene Fluoride–Trifluoroethylene–Chlorotrifluoroethylene) Terpolymers. *Macromolecules* **2015**, *48* (8), 2731–2739. https://doi.org/10.1021/acs.macromol.5b00185.

(40) Klein, R. J.; Runt, J.; Zhang, Q. M. Influence of Crystallization Conditions on the Microstructure and Electromechanical Properties of Poly(Vinylidene Fluoride−trifluoroethylene−chlorofluoroethylene) Terpolymers. *Macromolecules* **2003**, *36* (19), 7220–7226. https://doi.org/10.1021/ma034745b.

(41) Kolda, R. R.; Lando, J. B. The Effect of Hydrogen-Fluorine Defects on the Conformational Energy of Polytrifluoroethylene Chains. *Journal of Macromolecular Science, Part B* **1975**, *11* (1), 21–39. https://doi.org/10.1080/00222347508217853.

(42) Bargain, F.; Panine, P.; Domingues Dos Santos, F.; Tencé-Girault, S. From Solvent-Cast to Annealed and Poled Poly(VDF-Co-TrFE) Films: New Insights on the Defective Ferroelectric Phase. *Polymer* **2016**, *105*, 144–156. https://doi.org/10.1016/j.polymer.2016.10.010.

(43) Tashiro, K.; Kobayashi, M. Structural Phase Transition in Ferroelectric Fluorine Polymers: X-Ray Diffraction and Infrared/Raman Spectroscopic Study. *Phase Transitions* **1989**, *18* (3–4), 213–246. https://doi.org/10.1080/01411598908206864.

(44) Davis, G. T.; Furukawa, T.; Lovinger, A. J.; Broadhurst, M. G. Structural and Dielectric Investigation on the Nature of the Transition in a Copolymer of Vinylidene Fluoride and Trifluoroethylene (52/48 Mol %). *Macromolecules* **1982**, *15* (2), 329–333. https://doi.org/10.1021/ma00230a025.

(45) Lovinger, A. J.; Davis, G. T.; Furukawa, T.; Broadhurst, M. G. Crystalline Forms in a Copolymer of Vinylidene Fluoride and Trifluoroethylene (52/48 Mol %). *Macromolecules* **1982**, *15* (2), 323–328. https://doi.org/10.1021/ma00230a024.

(46) Tashiro, K.; Takano, K.; Kobayashi, M.; Chatani, Y.; Tadokoro, H. Structure and Ferroelectric Phase Transition of Vinylidene Fluoride-Trifluoroethylene Copolymers: 2. VDF 55% Copolymer. *Polymer* **1984**, *25* (2), 195–208. https://doi.org/10.1016/0032-3861(84)90326-4.

(47) Bellet-Amalric, E.; Legrand, J. F. Crystalline Structures and Phase Transition of the Ferroelectric P(VDF-TrFE) Copolymers, a Neutron Diffraction Study. *Eur. Phys. J. B* **1998**, *3* (2), 225–236. https://doi.org/10.1007/s100510050307.

(48) Krumova, M.; López, D.; Benavente, R.; Mijangos, C.; Pereña, J. M. Effect of Crosslinking on the Mechanical and Thermal Properties of Poly(Vinyl Alcohol). *Polymer* **2000**, *41* (26), 9265–9272. https://doi.org/10.1016/S0032-3861(00)00287-1.

(49) Taguet, A.; Ameduri, B.; Boutevin, B. Crosslinking of Vinylidene Fluoride-Containing Fluoropolymers. In *Crosslinking in Materials Science*; Advances in Polymer Science; Springer Berlin Heidelberg: Berlin, Heidelberg, 2005; pp 127–211. https://doi.org/10.1007/b136245.

(50) Chu, B.; Zhou, X.; Ren, K.; Neese, B.; Lin, M.; Wang, Q.; Bauer, F.; Zhang, Q. M. A Dielectric Polymer with High Electric Energy Density and Fast Discharge Speed. *Science* **2006**, *313* (5785), 334–336. https://doi.org/10.1126/science.1127798.

(51) Zhu, L. Exploring Strategies for High Dielectric Constant and Low Loss Polymer Dielectrics. *J. Phys. Chem. Lett.* **2014**, *5* (21), 3677–3687. https://doi.org/10.1021/jz501831q.

(52) Yang, L.; Tyburski, B. A.; Dos Santos, F. D.; Endoh, M. K.; Koga, T.; Huang, D.; Wang, Y.; Zhu, L. Relaxor Ferroelectric Behavior from Strong Physical Pinning in a Poly(Vinylidene Fluoride-Co-Trifluoroethylene-Co-Chlorotrifluoroethylene) Random Terpolymer. *Macromolecules* **2014**, *47* (22), 8119–8125. https://doi.org/10.1021/ma501852x.